Compensation and optimization of dispersion in nulling interferometry

J. F. P. Spronck, J. W. N. Los and S. F. Pereira,

Optics Research Group, Faculty of Applied Sciences,
Delft University of Technology,
Lorentzweg 1, NL-2628 CJ Delft, The Netherlands

ABSTRACT

The optical properties of materials are wavelength-dependent. This property, called *dispersion*, affects the performance of a wide-band nulling interferometer by inducing wavelength-dependent phase differences between the arms of the interferometer. In this paper, we analyze the influence of dispersion in nulling interferometers for exoplanet detection.

Keywords: Interferometry, Nulling interferometry, Dispersion, Astronomical optics, Exoplanet detection

1. INTRODUCTION

During the last decade, a large effort was spent on the search for exoplanets. Despite this effort, direct detection of an Earth-like exoplanet remains very challenging because of the huge brightness contrast between the star and the planet (10^6 in the best case) and their small angular separation (typically 0.1 arcsec). One promising candidate to meet this challenge is a technique called *nulling interferometry*.[1]

Nulling interferometry is a technique in which light coming from the on-axis star is cancelled by means of destructive interference between several beams. Light coming from a planetary companion would experience an additional phase difference between the beams due to the off-axis angular position of the planet. This additional phase difference would lead to a (partially) constructive interference for the companion. In order to detect an Earth-like exoplanet, the ratio between the intensities corresponding to constructive and destructive interference, the so-called *rejection ratio*, should be on the order of 10^6.

An additional requirement is that this high rejection ratio should be achieved for every wavelength in a wide spectral band (6–18 μm or even wider[2]). Indeed, such a broad band is needed in order to optimally exploit the photon flux coming from the planet and in order to obtain spectral information from the eventual planet atmosphere. To do so, most current nulling interferometers use an *achromatic phase shifter*.[3] There is also a family of nulling interferometers that makes use of chromatic phase shifters such as delay lines.[4,5]

The refractive index of a material is wavelength-dependent; this is called dispersion. In nulling interferometry, dispersion might be of great importance since all interfering beams will pass through different optics and might therefore acquire different wavelength-dependent phases. These different phases will affect the performance of the interferometer. Dispersion can be compensated for by adding some extra path lengths in glass. On the other hand, as we will see in this paper, dispersion could also be used to improve the performance of the interferometer and therefore could be used or optimized to reach a higher rejection ratio.

In Section 2, we analyze the effect of dispersion on the interference patterns and on the rejection ratio in the case of a two-beam nulling interferometer without achromatic phase shifters. In Section 3, we present the experimental set-up used to validate our theoretical findings. In Section 4, we show the experimental validation obtained with our table-top experimental set-up. Our conclusions are then summarized in Section 5.

E-mail: J.F.P.Spronck@tudelft.nl

Optical and Infrared Interferometry, edited by Markus Schöller, William C. Danchi, Françoise Delplancke
Proc. of SPIE Vol. 7013, 70131Q, (2008) · 0277-786X/08/$18 · doi: 10.1117/12.789298

2. THEORY AND SIMULATIONS

In this section, we will see how dispersion can affect the performance of a two-beam interferometer.

We consider two beams of amplitudes $a_1(\lambda)$ and $a_2(\lambda)$, with an achromatic phase difference $\Delta\phi$ and an optical path difference L between the two beams. Their complex amplitudes are given by

$$A_1(\lambda, L) = a_1(\lambda)\exp(i\Delta\phi), \tag{1a}$$

$$A_2(\lambda, L) = a_2(\lambda)\exp\left(i\frac{2\pi}{\lambda}L\right). \tag{1b}$$

If the second beam goes through an extra glass plate of thickness d and of refractive index $n(\lambda)$, we have

$$A_1(\lambda, L) = a_1(\lambda)\exp(i\Delta\phi), \tag{2a}$$

$$A_2(\lambda, L) = a_2(\lambda)\exp\left\{i\frac{2\pi}{\lambda}[L + n(\lambda)d]\right\}. \tag{2b}$$

For a given thickness d, the intensity after beam combination as a function of the optical path difference L is given by

$$I(L) = \int \left| a_1(\lambda)\exp(i\Delta\phi) + a_2(\lambda)\exp\left\{i\frac{2\pi}{\lambda}[L + n(\lambda)d]\right\}\right|^2 d\lambda. \tag{3}$$

In the family of interferometers introduced by Mieremet,[4] a high rejection ratio is possible with mere delay lines as phase shifters. In this paper, we therefore assume that there is no additional phase difference between the beams ($\Delta\phi = 0$). Furthermore, we assume that the beams have equal amplitudes ($a_1(\lambda) = a_2(\lambda) = a(\lambda)$). In this case, Eq. (3) can be written as

$$\begin{aligned} I(L) &= \int |a(\lambda)|^2 \left|1 + \exp\left\{i\frac{2\pi}{\lambda}[L + n(\lambda)d]\right\}\right|^2 d\lambda \\ &= 4\int |a(\lambda)|^2 \cos^2\left\{\frac{\pi}{\lambda}[L + n(\lambda)d]\right\} d\lambda. \end{aligned} \tag{4}$$

In our simulations, we chose the refractive index $n(\lambda)$ of BK7 and for the amplitude $a(\lambda)$, we used the spectrum of the Xe arc light source used in our experimental set-up. Interference patterns corresponding to different thicknesses $d = 0, 4.8, 9.6$ and 14.4 μm are depicted in Figs. 1(a-d) respectively. When there is no additional glass plate (Fig. 1(a)), the pattern is symmetric with respect to the zero-OPD position ($I(L) = I(-L)$). As the thickness of the additional glass plate increases to $d = 4.8$ μm (Fig. 1(b)), the fringes become asymmetric. For further increase of the plate thickness (Fig. 1(c), $d = 9.6$ μm) the fringes become quasi-symmetric with respect to the minimum of the interference pattern. Finally, as the thickness gets larger (Fig. 1(d)), the fringes become again asymmetric.

In order to understand the effect of this asymmetry in the fringe contrast, we define the rejection ratio as being the ratio between the maximal and the minimal intensities of the interference pattern,

$$R = \frac{\max(I(L))}{\min(I(L))}. \tag{5}$$

The rejection ratio as a function of the thickness d of the glass plate is depicted in Fig. 2 (solid line). Note that negative values of the thickness d physically mean that the glass plate has been introduced in the first beam instead of the second one. We can see that the rejection ratio is minimal when there is no glass plate ($d = 0$ μm) and is maximal when the thickness of the glass plate is around 9.6 μm. The rejection ratios corresponding to the fringes of Fig. 1(a-d) are marked by the four dots in Fig. 2. In order to compare the theory with the experiment, we also plot in Fig. 2 (dash-dotted line) the rejection ratio when the two beams have slightly different spectra ($a_1(\lambda) \neq a_2(\lambda)$), using the values obtained with our experimental set-up.[6,7] In this case, the rejection ratio has the same overall shape but the peak values are lower.

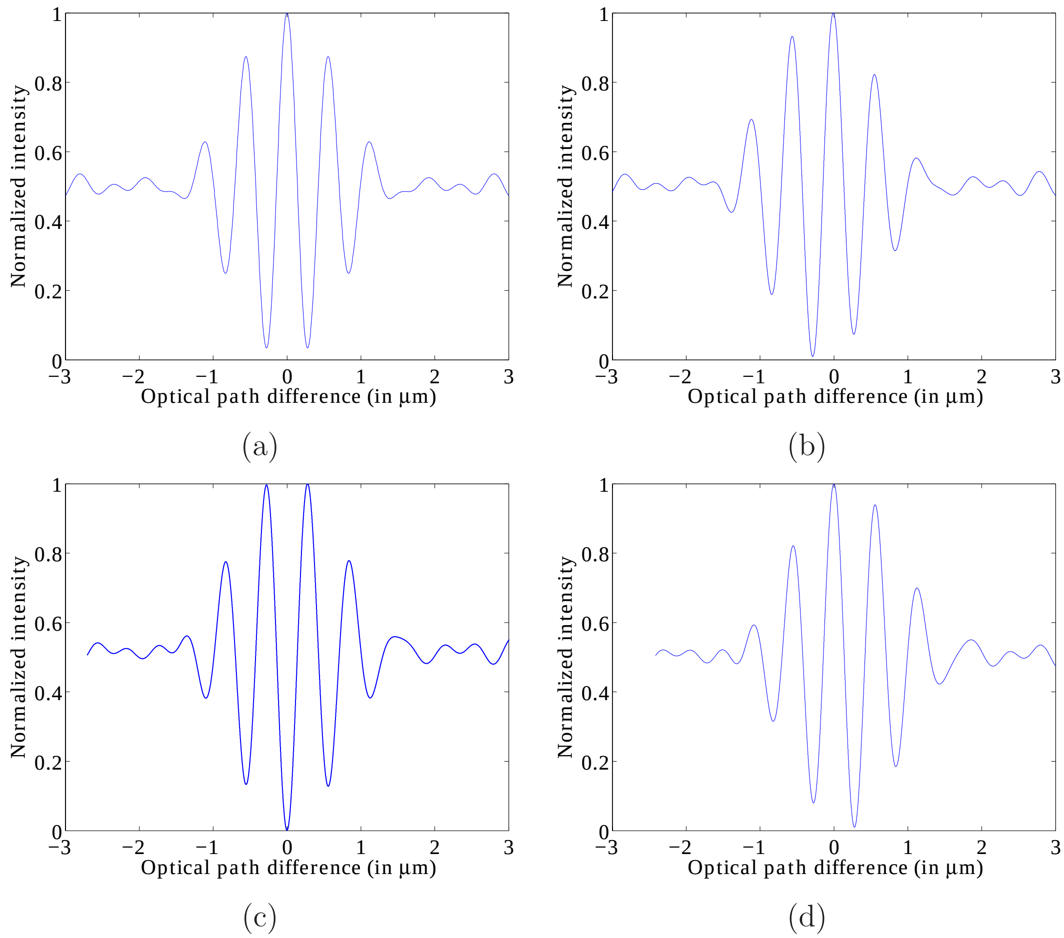

Figure 1. Interference patterns corresponding to different thicknesses of the glass plate: (a) $d = 0\mu$m, (b) $d = 4.8\mu$m, (c) $d = 9.6\mu$m and (d) $d = 14.4\mu$m.

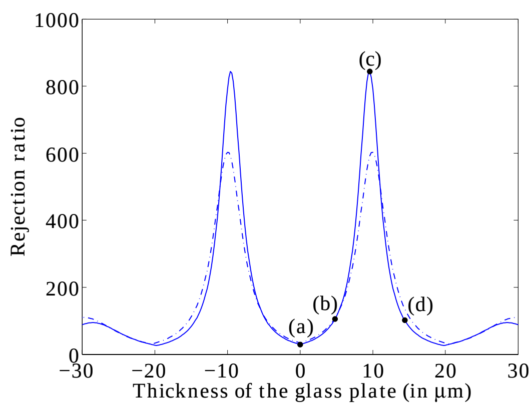

Figure 2. Rejection ratio as a function of the thickness of the introduced glass plate when there is no phase difference ($\Delta\Phi = 0$). For the solid lines, the spectrum of the two beams are identical and equal to the spectrum of the Xe lamp used in our experimental set-up and for the dash-dotted lines, the spectra of the beams are slightly different leading to a lower rejection ratio.

In order to understand why there is a peak in the rejection ratio, let us look at the phase difference between the two beams,

$$\Phi_2(\lambda) = \Phi_1(\lambda) + \frac{2\pi}{\lambda} L + \frac{2\pi}{\lambda} n(\lambda) d. \tag{6}$$

If we express the refractive index in a power series,

$$n(\lambda) = \sum_{j=0}^{\infty} \alpha_j \lambda^j, \tag{7}$$

we have

$$\Phi_2(\lambda) = \Phi_1(\lambda) + \frac{2\pi}{\lambda} L + \frac{2\pi}{\lambda} \alpha_0 d + \frac{2\pi}{\lambda} \alpha_1 \lambda d + \underbrace{\frac{2\pi}{\lambda} \sum_{j=2}^{\infty} \alpha_j \lambda^j}_{\mathcal{O}(\lambda)}. \tag{8}$$

After compensating for the optical path difference ($L = -\alpha_0 d$) and choosing the right thickness of the glass plate ($d = 1/2\alpha_1$), we find

$$\Phi_2(\lambda) = \Phi_1(\lambda) + \pi + \mathcal{O}(\lambda). \tag{9}$$

The glass plate acts therefore in this case as a first-order achromatic phase-shifter. Indeed, the fringes corresponding to the maximal rejection ratio (see Fig. 1(c)) are very similar to the one that would be obtained with an achromatic phase shifter.

When no achromatic phase shifter is present in the set-up, changing the dispersion can lead to a drastic increase in the rejection ratio. Indeed, we have seen that the rejection ratio without dispersion was minimal (of the order of 10^2 for two- and three-beam interferometers), while dispersion can lead to a rejection ratio orders of magnitude larger (10^3 for two beams and 10^5 for three beams). If we aim for the highest rejection ratio, one may conclude that additional dispersion should be used. However, on the other hand, in order to demonstrate the principle of nulling interferometry without achromatic phase shifter, as suggested in Ref. 8, one should compensate for differential dispersion.

3. EXPERIMENTAL SET-UP

In order to validate the theoretical predictions that we have made in the previous section, we performed measurements using our table-top experimental set-up. In this section, we describe the set-up.

The experimental set-up is depicted in Fig. 3. It is originally a modified Mach-Zehnder three-beam interferometer[6,7] but only two beams were used for these measurements. The set-up can be divided in three blocks: the star simulator (A), the interferometer (B) and the detection stage (C).

In the star simulator, light from a Xe arc lamp (LS) is focused onto an optical fiber (FB) via achromatic doublets (DB) in order to create a point source. Light coming out of the fiber is then collimated. For alignment purpose, we also use a He-Ne laser that we focus onto the same fiber using a folding mirror.

In the interferometer, two beams are created and then recombined with the help of four beam splitters. Each beam encounters, before recombination, a retro-reflector acting as a delay line. The optical path differences between the beams can be varied by changing the position of the delay lines (DL) with piezo-actuators.

After recombination, the beams are directed to a single-mode optical fiber for wavefront filtering. The fiber is then connected to a powermeter (DT) to detect the outcoming power. The interference pattern is then given by the measured intensity as a function of the position of the delay lines. We define the rejection ratio as the ratio between the maximum and the minimum of the interference pattern.

In order to see the influence of dispersion on the performance of the interferometer, a glass plate has been introduced in the path of each beam. The required difference in thickness between the two glass plates is of the order of a few microns. For simplicity, we used a 5 mm-thick BK7 plate in each beam that was rotated in order to achieve the desired differential path length in glass. An additional laser was used to measure the angle of

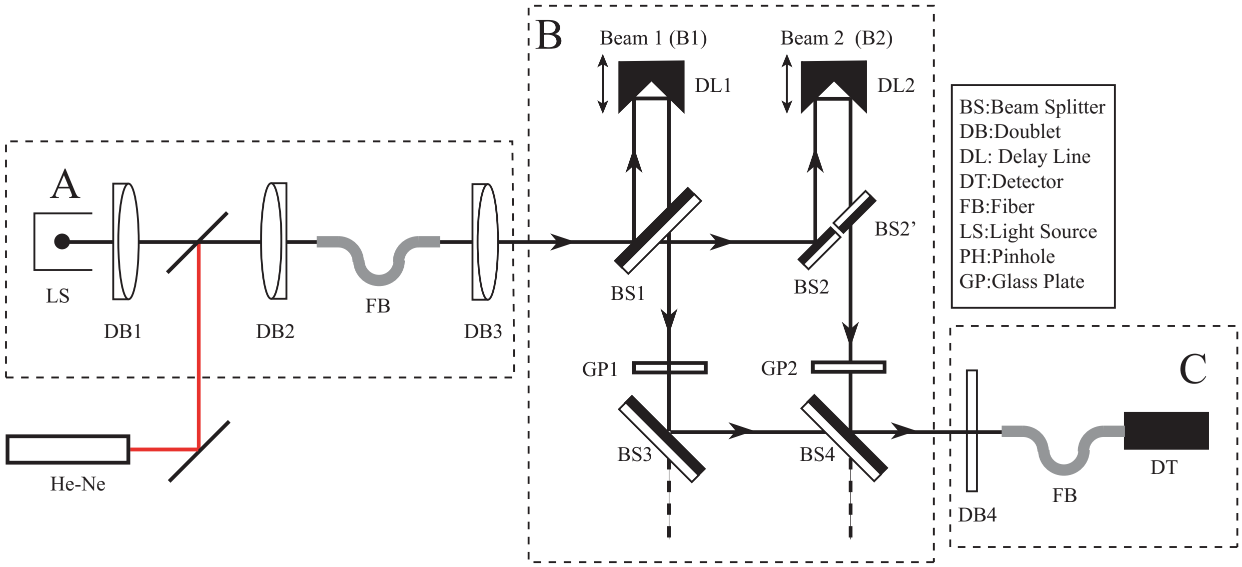

Figure 3. The experimental set-up can be divided in three blocks: the star-simulator (A), the interferometer (B) and the detection stage (C).

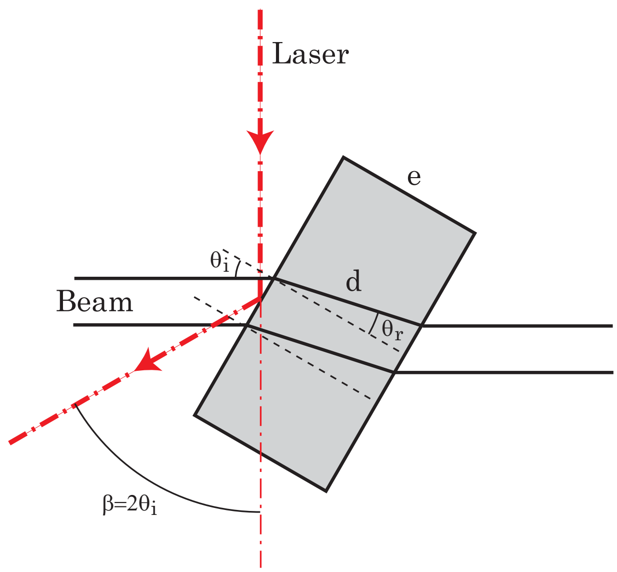

Figure 4. The path length of the beam inside the glass can be varied by rotation of the plate. A laser is used to measure the angle of rotation.

rotation $\beta = 2\theta_i$ of the plates (see Fig. 4). Using Snell's law, we can deduce the angle θ_r of the path of the beam inside the glass,

$$\theta_r = \arcsin\left(\frac{\sin\theta_i}{n}\right) = \arcsin\left[\frac{\sin(\beta/2)}{n}\right], \tag{10}$$

where n is the refractive index of the glass plate. The path length inside the glass is then given by

$$d = \frac{e}{cos\theta_r}, \tag{11}$$

where e is the thickness of the glass plate.

4. EXPERIMENTAL RESULTS

We performed measurements of the rejection ratio as a function of the differential thickness d. The results are depicted in Fig. 5. The overall shape is very similar to the one expected: a central minimum when there is no differential dispersion and two main peaks when the thickness increases followed by two secondary minima and secondary maxima. However, we can see that the position of the maxima and minima does not exactly coincide. This is probably due to slightly different spectra used in the simulations and in the experiment. Indeed, we used an additional filter to cut-off the infrared part of the spectrum. The final spectrum used in these measurements has not been measured. We also see that we found expected values for one of the maxima while significantly lower values have been found for the other maximum. This has been repeatedly measured and remains unexplained. A possible explanation would be the presence of additional non-compensated dispersion induced by the coatings of the beam-splitters and the mirrors, but this has to be confirmed.

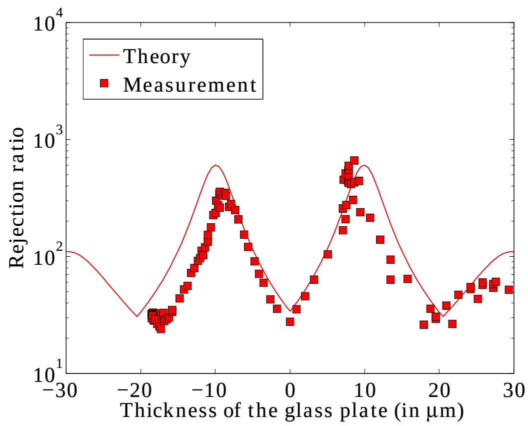

Figure 5. Measured rejection ratio as a function of the thickness of the glass plate d in the case of a nulling interferometer without achromatic phase shifter.

5. CONCLUSIONS

We have studied the effect of dispersion on the performances of two-beam nulling interferometer without achromatic phase shifters. We have seen that the rejection ratio will be minimal when there is no dispersion and the interference pattern will be symmetric with respect to the maximal intensity. Asymmetry will arise when introducing a glass plate in one of the beams. We have also concluded that if we carefully choose the thickness of the glass plate, we can realize a first-order achromatic phase shift that will lead to an optimal rejection ratio. Increasing further the plate thickness will decrease the rejection ratio to reach a secondary minimum etc.

We have seen that dispersion should be compensated for when the goal of the set-up is to demonstrate nulling interferometry without achromatic phase shifter. On the other hand, following the analysis presented in this paper, additional dispersion can be used in order to reach an optimal rejection ratio.

Finally, we have validated our theoretical predictions with measurements performed on our table-top experiment. We measured the rejection ratio as a function of the thickness of the introduced glass plate in the case of a nulling interferometer without achromatic phase shifter. The overall shape of the rejection ratio curve was in good agreement with the theory but the position of the minima and maxima did not exactly coincide, probably due a mismatch between the spectra used for the experiments and for the simulations.

With this study, we have shown that dispersion plays an important role in exoplanet detection by nulling interferometry since dispersion is unavoidable and since it affects the performance of the interferometer.

ACKNOWLEDGMENTS

The authors would like to acknowledge the support of TNO Science and Industry, The Netherlands.

REFERENCES

1. R. N. Bracewell, "Detecting nonsolar planets by spinning infrared interferometer," *Nature* **274**(5673), pp. 780–781, 1978.
2. J. R. Angel, A. Y. S. Cheng, and N. J. Woolf, "A space telescope for ir spectroscopy of earthlike planets," *Nature* **232**, pp. 341–343, 1986.
3. Y. Rabbia, J. Gay, J.-P. Rivet, and J.-L. Schneider, "Review of Concepts and Constraints for Achromatic Phase Shifters," in *GENIE - DARWIN Workshop - Hunting for Planets*, *ESA Special Publication* **522**, Mar. 2003.
4. A. L. Mieremet and J. J. M. Braat, "Deep nulling by means of multiple-beam recombination," *Appl. Opt.* **42**(10), pp. 1867–1875, 2003.
5. J. Spronck, S. Pereira, and J. Braat, "Chromatism compensation in wide-band nulling interferometry for exoplanet detection," *Appl. Opt.* **45**(4), pp. 597–604, 2006.
6. C. van der Avoort, A. Mieremet, S. Pereira, and J. Braat, "Demonstration of nulling using delay line phase shifters," *Proc. SPIE* **5491**(0), pp. 808–815, 2004.
7. J. Spronck, S. Pereira, and J. Braat, "Nulling interferometry without achromatic phase shifters: latest results," *Proc. SPIE* **6268**(0), p. 626832, 2006.
8. A. Mieremet and J. Braat, "Nulling interferometry without achromatic phase shifters," *Appl. Opt.* **41**(22), pp. 4697–4703, 2002.